Int. J. Solids Structures Vol. 18, No. 7, pp. 563–585, 1982
Printed in Great Britain.

0020-7683/82/070563-23$03.00/0

RELIABILITY OF AXIALLY COMPRESSED CYLINDRICAL SHELLS WITH RANDOM AXISYMMETRIC IMPERFECTIONS†

ISAAC ELISHAKOFF
Department of Aeronautical Engineering, Technion–Israel Institute of Technology, Haifa, Israel

and

JOHANN ARBOCZ
Department of Aerospace Engineering, Delft University of Technology, Delft, The Netherlands

(*Received* 26 *November* 1980; *in revised form* 8 *June* 1981)

Abstract—The paper is concerned with the effect of random axisymmetric imperfections on the buckling of circular cylindrical shells under axial compression. The initial imperfections are considered as random functions of the axial coordinate. This is done by expanding them in terms of the buckling modes of the associated perfect structure, and then treating the Fourier coefficients as random variables.

Initially the probabilistic properties of the initial imperfections of cylindrical shells, produced by the same manufacturing process, are studied. In contrast to earlier works the probabilistic properties (the mean function and the autocorrelation function or the spectral density) are not assumed. The mean vector and the variance–covariance matrix of the Fourier coefficients are calculated from experimental measurements of the shell profiles.

Next the Monte Carlo Method is applied. The Fourier coefficients of the initial imperfection representations are simulated by a special numerical procedure. Thus large number of shells is "created". For each shell a deterministic analysis of buckling stress evaluation is carried out. Finally, the reliability function representing the probability (i.e. fraction of an ensemble) of the buckling stress exceeding the specified stress is calculated. The reliability function permits to evaluate the design stress for the whole ensemble of shells produced by a given manufacturing process, defined as the stress level for which the desired reliability is achieved. The paper represents an extension of the approach given in Ref. [1] to shell structures.

1. INTRODUCTION

The considerations which follow are intended as a contribution to the understanding of the random imperfection-sensitivity of shell structures. Specifically, we are dealing with a circular cylindrical shell under uniform axial compression, with the axisymmetric imperfections treated as random functions of the axial coordinate. This study generalizes a recent paper[1] where buckling of a model structure, that of a column on a cubic foundation was studied, and it should be considered as the initial step towards the analysis of shells with general, non-symmetric random imperfactions.

It has been believed for some time that the theories of imperfection-sensitivity of structures should be combined with the statistical analysis of the initial imperfections. The first work in this direction for the most controversial structure—the circular cylindrical shell under axial compression—was presented by Amazigo[2]. He treated infinitely long cylindrical shells with homogeneous, ergodic random axisymmetric imperfections by means of a modified truncated hierarchy method. The conclusion derived was that the buckling stress is a deterministic quantity, depending only on the spectral density of the random axisymmetric imperfections. Moreover, for small values of the standard deviations of the initial imperfections this deterministic buckling stress depended only on the value of the initial imperfection power spectral density at the spatial frequency of the classical axisymmetric buckling mode, this dependence being

$$\lambda = 1 - \left[\frac{9\pi c^2}{2\sqrt{2}}\,\bar{S}_{w_0}(1)\right]^{2/7}\delta^{4/7}, \quad \lambda = \frac{P_{BIF}}{P_C} \tag{1}$$

where P_{BIF} is the buckling load at which the governing nonlinear equations admit an asymmetric solution infinitesimally adjacent to the prebuckling axisymmetric state, P_C is the classical

†Presented at Euromech Colloquium No. 128: "Stability, Buckling and Postbuckling Behaviour: Foundations and Analysis", 31 March–2 April 1980, Delft, The Netherlands.

buckling load of the perfect structure, λ is the nondimensional deterministic buckling load (and therefore also the mean buckling load), $c = [3(1-\nu^2)]^{1/2}$, ν-Poisson's ratio, $\bar{S}_{W_0}(\omega)$-normalized initial axisymmetric imperfection power spectral density so that $\int_{-\infty}^{\infty} \bar{S}_{W_0}(\omega)\,d\omega = 1$, ω-the nondimensional spatial frequency so that $\omega = 1$ corresponds to the wave number associated with the axisymmetric buckling mode, δ is the standard deviation of the initial imperfections. In Ref. [3], Amazigo and Budiansky modified eqn (1) to

$$\lambda = 1 - \left[\frac{9\pi c^2}{2\sqrt{2}}\,\bar{S}_{W_0}(1)\right]^{2/7} \delta^{4/7}\lambda^{4/7}. \tag{2}$$

In Refs. [2–4], the normalized autocorrelation function $\bar{R}_{W_0}(x_1, x_2) = R_{W_0}(x_1, x_2)\delta^{-2}$ was assumed to be of exponential-cosine type

$$\bar{R}_{W_0}(x_1, x_2) = e^{-\beta|\eta|}\cos\gamma\eta \tag{3}$$

where η is the difference between the nondimensional axial coordinates of the points of observation, β and γ are some positive constants supposed to depend on the manufacturing process. The normalized spectral density associated with this autocorrelation function is

$$\bar{S}_{W_0}(\omega) = \frac{\beta}{\pi}\,\frac{\omega^2 + \omega^2 + \gamma^2}{\omega^4 + 2(\beta^2 - \gamma^2)\omega^2 + (\beta^2 + \gamma^2)^2} \tag{4}$$

so that $\bar{S}_{W_0}(1)$ entering into eqns (1) and (2) is

$$\bar{S}_{W_0}(1) = \frac{\beta}{\pi}\,\frac{1 + \beta^2 + \gamma^2}{1 + 2(\beta^2 - \gamma^2) + (\beta^2 + \gamma^2)^2}. \tag{5}$$

A design criterion based on formula (2) was developed by Tennyson *et al.*[4]. Two approaches were suggested: to substitute the experimentally determined values of δ and $\bar{S}_{W_0}(1)$ into eqn (2) or to assume, as in Refs. [2, 4] the exponential–cosine autocorrelation function (3) with parameters β and γ chosen so that the spectral density (4) will have a peak at the spatial frequency which corresponds to the axisymmetric classical buckling mode of the perfect shell. Experimental results[5] however, did not yield good agreement with the proposed random axisymmetric imperfection model, since the measured discrete power spectral density of initial imperfections did not have a peak at the spatial frequency which corresponds to the axisymmetric classical buckling mode of the perfect shell. A different approach was used by Roorda and Hansen[6]. They assumed that the shape of the initial imperfection was specified in the form of the axisymmetric buckling mode of the cylindrical shell and considered its magnitude as a random variable with given probability distribution. Then the following relationship derived by Koiter[7] using his general nonlinear theory of elastic stability

$$2(1-\lambda)^2 - 3c|\mu|\lambda = 0 \tag{6}$$

between the nondimensional buckling load λ and the magnitude of nondimensional imperfection μ was used as a transfer function to calculate the probability characteristics of buckling load in terms of the probability characteristics of the imperfection magnitude. Finally the reliability function

$$R(\alpha) = \text{Prob}\,(\alpha < \Lambda \leqq 1) \tag{7}$$

where $(\alpha < \Lambda \leqq 1)$ stands for the random event that the random buckling load Λ will exceed given nondimensional load α, was calculated.

In a subsequent paper[8] Roorda proposed to consider all kinds of imperfections in a real shell of given length, radius, thickness and boundary conditions to be equivalent to a hypothetical axisymmetric imperfection in a shell of infinite length with the same radius and thickness. This equivalent imperfection was treated as a random normal variable with its mean

and variance approximated as linear function of the R/t ratio. The obtained formulas were compared with results of some 360 experiments on axially compressed cylindrical shells with different length, radius-to-thickness ratios, boundary conditions, materials and manufacturing processes, which were reported in Ref. [9]. Roorda also compared his results with the "lower bound" curve proposed by Weingarten *et al.*[10] for a large number of test results from different sources.

Makaroff[11] was apparently the first who performed at the Moscow Energy Institute systematic statistical analysis of the initial imperfections. He used series of fifty cylindrical shells made of steel sheet of electrical-grade pressboard. The imperfection function was represented in Fourier series and the coefficients were treated as random variables. The analysis showed that the assumption of homogeneity of the initial imperfection in the circumferential direction was satisfactory, and that the normality of their Fourier coefficients did not conflict with the experimental data. Subsequently, Makaroff[12] performed a theoretical analysis of the buckling of stochastically imperfect shells with the experimental data obtained in Ref. [11] serving as an input for the description of imperfections. The theoretical mean value of the nondimensional buckling load was 0.31 whereas the experiments yielded 0.23.

General, nonaxisymmetric random imperfections were treated by Fersht[13] and Hansen[14]. Fersht generalized the approach by Amazigo[2]. It turned out, that for the nonaxisymmetric imperfections closed formulas of the type (1) or (2) are not obtainable and rather cumbersome numerical analysis has to be performed to yield the mean buckling load. Hansen[14] generalized his previous deterministic results given in Ref.[15]. The main conclusion of Ref. [15] was that the imperfection parameters associated with the non-axisymmetric modes appear only in three and only three distinct summations and that the system behaviour is governed by the value of these summations and not by the individual imperfection parameters. It was assumed that the modal imperfection amplitudes are jointly normal random variables with zero mean. Also the strong assumption was made that these amplitudes are statistically independent and are distributed identically. The Monte Carlo Method was then applied: for each sample problem the buckling load was determined via Ref. [15], and the mean buckling loads as well as their confidence levels were calculated. It has been demonstrated that the non-axisymmetric imperfections play a very important role in the determination of the buckling load statistics. Another important conclusion was that the large dispersion occurs for small values of R/t and that this dispersion decreases as R/t increases. The same conclusion was accounted for by Roorda[8] by postulating that the mean and the variance of the imperfection were functions decaying with increasing values of R/t.

In this paper, contrary to earlier works, the probabilistic properties (the autocorrelation functions or spectral densities) are not assumed, but the mean vector and the variance–covariance matrix of the Fourier coefficients are calculated from the experimental measurements of the shell profiles. Then the Monte Carlo Method is employed. Thus, at first, a large number of shells is "created". That is, the Fourier coefficients of their initial imperfection representations are simulated numerically by a special procedure. Next for each shell a deterministic analysis of buckling load evaluation is carried out (implying that the usual deterministic approach is a particular case of the probabilistic one). Once the buckling loads of an ensemble of shells are available one then proceeds by studying their probabilistic behaviour. In particular, one determines the reliability function representing the relative number of shells with buckling loads exceeding the specified load. Finally, the design load for the shells produced by a given manufacturing process is obtained as that load for which the reliability function has the desired value close to unity.

2. PROBABILISTIC PROPERTIES OF INITIAL IMPERFECTIONS

We characterize the random initial imperfections W_0 by functions which are basis in the study of random processes. The mean function $\bar{W}_0(x)$ of a function W_0 is the expected value of the random variable $W_0(x)$

$$\bar{W}_0(x) = E\{W_0(x)\} = \int_{-\infty}^{\infty} w_0 f(w_0; x)\, \mathrm{d}w_0 \tag{8}$$

where $f(w_0; x)$ is the first-order probability density function of $W_0(x)$. In general, $\tilde{W}_0(x)$ is a function of the axial coordinate, and $E\{\ldots\}$ denotes the mathematical expectation. The autocovariance function $R_{W_0}(x_1, x_2)$ of a random function $W_0(x)$ is the covariance of the random variables $W_0(x_1)$ and $W_0(x_2)$:

$$\begin{aligned} R_{W_0}(x_1, x_2) &= E\{[W_0(x_1) - \tilde{W}_0(x_1)][W_0(x_2) - \tilde{W}_0(x_2)]\} \\ &= \int_{-\infty}^{\infty}\int_{-\infty}^{\infty} [w_{01} - \tilde{W}_0(x_1)][w_{02} - \tilde{W}_0(x)] \\ &\quad \times f(w_{01}, w_{02}; x_1, x_2)\, \mathrm{d}w_{01}\, \mathrm{d}w_{02} \end{aligned} \tag{9}$$

where $f(w_{01}, w_{02}; x_1, x_2)$ is the second-order probability density of the random function $W_0(x)$. Assume now that $\{\varphi_i(x)\}$ represents the complete set of orthogonal functions in $[0, L]$, where L is the shell length. Then $W_0(x)$ can be expanded in a series in terms of the $\varphi_i(x)$'s:

$$W_0(x) = \sum_i A_i \varphi_i(x) \tag{10}$$

where A_i is a random variable for every fixed i. The mean function then becomes

$$\tilde{W}_0(x) = \sum_i E(A_i)\varphi_i(x), \qquad E(A_i) \equiv \tilde{A}_i. \tag{11}$$

Here the $\tilde{A}_i$'s are the means of the A_i's and are readily found as

$$\tilde{A}_i = \frac{1}{\mu_i^2}\int_0^L \tilde{W}_0(x)\varphi_i(x)\, \mathrm{d}x, \qquad \mu_i^2 = \int_0^L \varphi_i^2(x)\, \mathrm{d}x \tag{12}$$

and they form the mean vector $\{\tilde{A}\}$. The autocovariance function becomes, correspondingly,

$$R_{W_0}(x_1, x_2) = \sum_i \sum_j \sigma_{ij}\varphi_i(x_1)\varphi_j(x_2) \tag{13}$$

where

$$\sigma_{ij} = E\{[A_i - \tilde{A}_i][A_j - \tilde{A}_j]\}. \tag{14}$$

The σ_{ij}'s are obtained as

$$\sigma_{ij} = \frac{1}{\mu_i^2 \mu_j^2}\int_0^L \int_0^L R_{W_0}(x_1, x_2)\varphi_i(x_1)\varphi_j(x_2)\, \mathrm{d}x_1\, \mathrm{d}x_2 \tag{15}$$

and they form the variance–covariance matrix $[\Sigma] = [\sigma_{ij}]$. The equations (8)–(15) imply, that the knowledge of the mean and the autocovariance function on the one hand, and the mean vector $\{\tilde{A}\}$ and the variance–covariance matrix $[\Sigma]$ on the other, are equivalent.

In order to be able to treat also the limiting case of the infinite shell, we consider initially the complex Fourier series, so that instead of representation (10) we use

$$W_0(x) = \sum_{m=-\infty}^{\infty} A_m\, \mathrm{e}^{im\pi x/L}. \tag{16}$$

For the mean function we get

$$\tilde{W}_0(x) = \sum_{m=-\infty}^{\infty} E(A_m)\mathrm{e}^{im\pi x/L}, \tilde{A}_m = \frac{1}{2L}\int_{-L}^{L} \tilde{W}_0(s)\, \mathrm{e}^{-im\pi s/L}\, \mathrm{d}s. \tag{17}$$

The autocovariance function becomes in terms of the elements σ_{mn} of the variance–covariance matrix

$$R_{W_0}(x_1, x_2) = \sum_{m=-\infty}^{\infty} \sum_{n=-\infty}^{\infty} \sigma_{mn} \, e^{i\pi(mx_1 - nx_2)/L}$$

$$\sigma_{mn} = \frac{1}{4L^2} \int_{-L}^{L} \int_{-L}^{L} R_{W_0}(s_1, s_2) \, e^{i\pi(-ms_1 + ns_2)/L} \, ds_1 \, ds_2. \tag{18}$$

Substitution of the σ_{mn} into the expression of the autocovariance function yields

$$R_{W_0}(x_1, x_2) = \sum_{m=-\infty}^{\infty} \sum_{n=-\infty}^{\infty} \left[\frac{1}{4L^2} \int_{-L}^{L} \int_{-L}^{L} R_{W_0}(s_1, s_2) \, e^{-im\pi s_1/L} \right.$$

$$\left. \times e^{in\pi s_2/L} \, ds_1 \, ds_2 \right] e^{im\pi x_1/L} \, e^{-in\pi x_2/L}. \tag{19}$$

Now, defining the spatial frequencies by

$$\omega_m = \frac{m\pi}{L}, \quad \omega_n = \frac{n\pi}{L} \tag{20}$$

and the difference between the successive frequencies by

$$\Delta\omega_m = \frac{\pi}{L}, \Delta\omega_n = \frac{\pi}{L} \tag{21}$$

Equation (19) becomes

$$R_{W_0}(x_1, x_2) = \sum_{m=-\infty}^{\infty} \sum_{n=-\infty}^{\infty} \left[\frac{1}{4\pi^2} \int_{-L}^{L} \int_{-L}^{L} R_{W_0}(s_1, s_2) \, e^{-i\omega_m s_1} \, e^{i\omega_n s_2} \, ds_1 \, ds_2 \right]$$

$$\times e^{i\omega_m x_1} \, e^{-i\omega_n x_2} \, \Delta\omega_m \Delta\omega_n. \tag{22}$$

If we now define

$$S_{W_{0,L}}(\omega_m, \omega_n) = \frac{1}{4\pi^2} \int_{-L}^{L} \int_{-L}^{L} R_{W_0}(s_1, s_2) \, e^{-i\omega_m s_1} \, e^{i\omega_n s_2} \, ds_1 \, ds_2 \tag{23}$$

then eqn (22) can be rewritten as follows

$$R_{W_0}(x_1, x_2) = \sum_{m=-\infty}^{\infty} \sum_{n=-\infty}^{\infty} S_{W_{0,L}}(\omega_m, \omega_n) \, e^{i\omega_m x_1} \, e^{-i\omega_n x_2} \Delta\omega_m \Delta\omega_n. \tag{24}$$

Under very general conditions the limit of a sum of the form (24) as $\Delta\omega_m \to 0$, $\Delta\omega_n \to 0$ is the integral

$$R_{W_0}(x_1, x_2) = \int_{-\infty}^{\infty} \int_{-\infty}^{\infty} S_{W_0}(\omega_1, \omega_2) \, e^{i\omega_1 x_1} \, e^{-i\omega_2 x_2} \, d\omega_1 \, d\omega_2. \tag{25}$$

Therefore, since $L \to \infty$ implies $\Delta\omega_m \to 0$, $\Delta\omega_n \to 0$ we have

$$\lim_{L\to\infty} S_{W_{0,L}}(\omega_m, \omega_n) = S_{W_0}(\omega_1, \omega_2)$$

where

$$S_{W_0}(\omega_1, \omega_2) = \frac{1}{4\pi^2} \int_{-\infty}^{\infty} \int_{-\infty}^{\infty} R_{W_0}(s_1, s_2)\, e^{-i\omega_1 s_1}\, e^{i\omega_2 s_2}\, ds_1\, ds_2 \tag{26}$$

so that $S_{W_0}(\omega_1, \omega_2)$ and $R_{W_0}(s_1, s_2)$ constitute the double Fourier transform pair. $S_{W_0}(\omega_1, \omega_2)$ is referred to as the generalized power spectral density of the initial imperfections of the infinite shell, and as was shown above, it can be deduced from the elements of the variance–covariance matrix associated with the finite shell.

Consider now the particular case when the initial imperfections of the finite shell form a stationary random function, meaning that the mean imperfection is constant and the auto-covariance depends only on $s_2 - s_1$:

$$\bar{W}_0(x) = \text{constant}, \quad R_{W_0}(x_1, x_1 + \xi) = R_{W_0}(\xi). \tag{27}$$

Substituting into eqn (26) $R_{W_0}(s_2 - s_1)$ instead of $R_{W_2}(s_1, s_2)$, making the change of coordinates

$$s_1 - s_2 = \xi, \quad s_2 = \eta$$

and bearing in mind that

$$\int_{-\infty}^{\infty} e^{i(\omega_2 - \omega_1)\eta}\, d\eta = 2\pi\delta(\omega_2 - \omega_1)$$

yields

$$S_{W_0}(\omega_1, \omega_2) = S_{W_0}(\omega_1)\delta(\omega_2 - \omega_1)$$

where $S_{W_0}(\omega_1)$ is the power spectral density of the weakly homogeneous initial imperfections (homogeneous in the wide-sense). Then with $\omega_1 \to \omega$ one obtains

$$S_{W_0}(\omega) = \frac{1}{2\pi} \int_{-\infty}^{\infty} R_{W_0}(\xi)\, e^{-i\omega\xi}\, d\xi \tag{28}$$

with eqn (25) transforming to

$$R_{W_0}(\xi) = \int_{-\infty}^{\infty} S_{W_0}(\omega)\, e^{i\omega\xi}\, d\omega \tag{29}$$

eqns (28) and (29) constitute the Wiener–Khintchine relationship for the weakly homogeneous random functions. The concept of the power spectral density was used in the studies by Amazigo [2] and Amazigo and Budiansky [3] to represent the initial imperfections.

Strictly speaking, the initial imperfections of the finite shell cannot be stationary. Tennyson *et al.* [4] used measurements performed on the finite shell in order to develop the design criterion based on formula (2) which was derived from the infinite shell with weakly stationary imperfections. That is, the assumption was made that the initial imperfections are stationary in the interval $[0, L]$, i.e. conditions (27) are valid when x_1, x_2 belong to this interval. Consider this case in more detail. Assume, after Tennyson *et al.* [4] that the mean imperfection function is identically zero. Then the initial imperfections (as those of the finite shell) are characterized by the variance–covariance matrix eqn (14). Assume now in eqn (15) that $R_{W_0}(s_1, s_2) = R_{W_0}(s_2 - s_1)$ and introduce a new coordinate system $z_1 = (s_2 - s_1)/\sqrt{2}$, $z_2 = (s_1 + s_2)/\sqrt{2}$ to arrive finally at

$$\sigma_{mn} = \frac{(-1)^{n-m}}{\pi(n-m)} \int_0^1 R_{W_0}(2\alpha L)(\sin 2m\pi\alpha - \sin 2n\pi\alpha)\, d\alpha, \quad \text{if } m \neq n \tag{30}$$

and

$$\sigma_{mn} = 2\int_0^1 R_{W_0}(2\alpha L)(1-\alpha)\cos 2m\pi\alpha \, d\alpha, \quad \text{if } m = n$$

where

$$\alpha = \frac{z_1}{\sqrt{2L}} = \frac{s_2 - s_1}{2L} = \frac{\gamma}{2L}. \tag{31}$$

We will show that for $L \to \infty$, the diagonal terms σ_{mm} of the variance–covariance matrix reduce to Tennyson's discrete power spectral density. Indeed, substituting (31) into the expression for σ_{mm}, results in

$$\sigma_{mm} = \frac{1}{L}\int_0^{2L} R_{W_0}(\gamma)\left(1 - \frac{\gamma}{2L}\right)\cos m\omega_0\gamma \, d\gamma$$

where the dimensional spatial frequency $\tilde{\omega}_0 = \pi/L$ was introduced. Then

$$\frac{\sigma_{mm}}{\tilde{\omega}_0} = \frac{1}{\pi}\int_0^{2L} R_{W_0}(\gamma)\left(1 - \frac{\gamma}{2L}\right)\cos m\tilde{\omega}_0\gamma \, d\gamma$$

but now, with $L \to \infty$, $\tilde{\omega}_0 \to 0$ and

$$\lim_{\tilde{\omega}_0 \to 0} m\tilde{\omega}_0 = \tilde{\omega}$$

hence

$$\lim_{\tilde{\omega}_0 \to 0} \frac{\sigma_{mm}}{\tilde{\omega}_0} = \frac{1}{\pi}\int_0^{\infty} R_{W_0}(\gamma)\cos\tilde{\omega}\gamma \, d\gamma = S_{W_0}(\tilde{\omega}) \tag{32}$$

which is the desired result. This expression can be related also to the nondimensional discrete power spectral density discussed in Ref. [16]. Indeed $S_{W_0}(\tilde{\omega})$ in the notation of Ref. [16] is $p(\tilde{\omega})$. In order to nondimensionalize $S_{W_0}(\tilde{\omega})$ we introduce the dimensionless spatial frequency ω defined as

$$\omega = \frac{m\tilde{\omega}_0}{\sqrt{(2c/Rt)}} = \frac{m}{i_{cl}}, \quad i_{cl} = \frac{L}{\pi}\sqrt{\left(\frac{2c}{Rt}\right)}$$

where i_{cl} is the number of half waves in the classical axisymmetric buckling mode for isotropic shells. Then the nondimensional power spectral density $\bar{S}_{W_0}(\omega) = S_{W_0}(\tilde{\omega})/\sqrt{(Rt/2c)}$ becomes

$$\bar{S}_{W_0}(\omega) = \frac{1}{\sqrt{(Rt/2c)}} \lim_{\tilde{\omega}_0 \to 0} \frac{\sigma_{mm}}{\tilde{\omega}_0} = \lim_{\tilde{\omega}_0 \to 0} \sigma_{mm} i_{cl} \tag{33}$$

which coincides with formula (A12) in Ref. [16].

3. SIMULATION OF RANDOM IMPERFECTIONS WITH GIVEN PROBABILISTIC PROPERTIES

Assume that the mean function $\bar{W}_0(x)$ and the autocovariance function $R_{W_0}(x_1, x_2)$ are given. We then calculate analytically or numerically the vector $\{\tilde{A}\}$ and the variance–covariance matrix $[\Sigma]$. Having these quantities, we then proceed to the simulation of the initial imperfections. Our aim is to "create" the desired number M of initial imperfection profiles having given probabilistic properties. The method of simulation, suitable for computer realization for a random normal function was developed in Ref. [17]. Here we are only giving a short outline of the method. We assume that the mean vector $\{\tilde{A}\}$ is identically zero. This entails no loss of

generality since if vector $\{A\}$ is simulated as below, the vector $\{A + \tilde{A}\}$ has the mean $\{\tilde{A}\}$ and the same variance-covariance matrix $[\Sigma]$. The latter matrix is positive semidefinite and can be uniquely decomposed in the form

$$[\Sigma] = [C][C]^T \tag{34}$$

where T means transpose and $[C]$ is a lower-triangular matrix. $[C]$ is found by the Cholesky's algorithm. Now, we form vector $\{B\}$, its elements being normally distributed, statistically independent with zero means and unit variances. Then the vector of the Fourier coefficients of the initial imperfections is simulated as follows:

$$\{A\} = [C]\{B\} + \{\tilde{A}\}. \tag{35}$$

Having M realizations of vector $\{B\}$ we obtain the same number of realizations of $\{A\}$. The main feature of this simulation technique is that it is applicable for homogeneous, as well as for nonhomogeneous random functions with given mean and autocovariance functions. This procedure was applied to different static and dynamic buckling problems, involving random imperfection sensitivity, in Refs. [1, 18, 19].

Using the autocovariance function (3) we are able to compare the results of the Monte Carlo Method with the expressions (1) or (2) for the mean buckling load. To begin with, we assume, after Amazigo[2], that the initial imperfection autocovariance function is of the exponential–cosine type

$$R_{W_0}(x_1, x_2) = \delta^2 \, \mathrm{e}^{-A(|x_2 - x_1|/L)} \cos B \frac{(x_2 - x_1)}{L}. \tag{36}$$

In order to get Amazigo's representation in the form of eqn (3) the constants A and B must have the following values.

$$A = \beta i_{cl} \pi, \quad B = \gamma i_{cl} \pi \tag{37}$$

where

$$i_{cl} = \frac{L}{\pi} \frac{\sqrt{2c}}{RT} \text{ and } c = \sqrt{[3(1 - \nu^2)]} \tag{38}$$

(See Appendix A for the details.)†

The elements of the variance–covariance matrix are calculated via eqn (15), with $\varphi_i = \cos(i\pi x/L)$, i.e. the half-wave cosine representation is used for the initial imperfections. As is shown in Ref. [18], simplification during calculating σ_{ij} is possible due to the weak homogeneity of W_0. Namely the σ_{ij}'s are given by

$$\sigma_{ij} = \frac{1}{\mu_i^2 \mu_j^2} \int_0^L R_{W_0}(\xi) M_{ij}(\xi) \, \mathrm{d}\xi \tag{39}$$

where

$$M_{ij}(\xi) = P_{ij}(\xi) + P_{ji}(\xi), \quad \mu_i^2 = \int_0^L \varphi_i^2(x) \, \mathrm{d}x$$

$$P_{ij}(\xi) = \int_{\xi/2}^{L - \xi/2} \varphi_i(\eta - \tfrac{1}{2}\xi) \varphi_i(\eta + \tfrac{1}{2}\xi) \, \mathrm{d}\eta$$

(see eqns (18)–(20) in Ref. [17]). These equations yield upon substitution and carrying out of the

†Appendices are included in Ref. [27], which represents an extended version of this paper.

integrals the following formulas

$$\bar{\sigma}_{ii} = \sigma_{ii} i_{cl} = \frac{4\delta^2}{\pi} \frac{\Omega_i}{\omega_i^4 + 2\omega_i^2(\beta^2 - \gamma^2) + (\beta^2 + \gamma^2)^2}$$

$$\bar{\sigma}_{ij} = \sigma_{ij} i_{cl} = \begin{cases} \dfrac{8\delta^2}{i_{cl}} \dfrac{(\omega_i^2 \bar{A}_i - \omega_j^2 \bar{A}_j)}{\omega_i^2 - \omega_j^2}, & \text{if } i \neq j \text{ and } i + j = \text{even} \\ 0, & \text{if } i + j = \text{odd} \end{cases} \tag{40}$$

where

$$\Omega_i = \beta \bar{U}_i - \frac{1}{2\pi i_{cl}} \left(\frac{\bar{P}_i \bar{Q}_i}{\bar{R}_i} + \frac{\bar{T}_i \bar{R}_i}{\bar{Q}_i} + 2\bar{V}_i \right) [1 - (-1)^i \, e^{-\beta i_{cl} \pi} \cos \gamma i_{cl} \pi]$$

$$- \frac{\beta}{\pi i_{cl}} \left[\frac{(\omega_i + \gamma)\bar{Q}_i}{\bar{R}_i} - \frac{(\omega_i - \gamma)\bar{R}_i}{\bar{Q}_i} + 2\gamma \right] (-1)^i \, e^{-\beta i_{cl} \pi} \sin \gamma i_{cl} \pi$$

$$\bar{A}_i = \frac{1}{\pi^2} \frac{1}{\omega_i^4 + 2\omega_i^2(\beta^2 - \gamma^2) + (\beta^2 + \gamma^2)^2}$$

$$\times \{ \bar{V}_i [(-1)^i \, e^{-\beta i_{cl} \pi} \cos \gamma i_{cl} \pi - 1] +$$

$$- 2\beta\gamma (-1)^i \, e^{-\beta i_{cl} \pi} \sin \gamma i_{cl} \pi \}$$

$$\bar{P}_i = \beta^2 - (\omega_i + \gamma)^2, \; \bar{Q}_i = \beta^2 + (\omega_i - \gamma)^2$$

$$\bar{R}_i = \beta^2 + (\omega_i + \gamma)^2, \; \bar{T}_i = \beta^2 - (\omega_i - \gamma)^2$$

$$\bar{U}_i = \omega_i^2 + \beta^2 + \gamma^2, \; \bar{V}_i = \omega_i^2 + \beta^2 - \gamma^2$$

$$\omega_i = i / i_{cl}. \tag{41}$$

In order to compare the results of the Monte Carlo Method with those obtained by the application of the formulas (1) and (2) the following shell was used: $R = L = 101.6$ mm, $t = 0.944931$ mm and $\nu = 0.3$ resulting in $i_{cl} = 6$. This shell, with the initial imperfection autocovariance function used by Amazigo (see eqn (3) with $\beta = 0.2$ and $\gamma = 1.0$), will be referred to as the Amazigo shell. Figure 1 shows the normalized variance of the initial imperfections back-calculated with the aid of the σ_{ij}'s given in eqn (40). Twelve terms have been retained in the summation given by eqn (13). The uniformity is disturbed in the vicinity of the edges due to Gibb's phenomenon. The autocovariance function possessed by 100 simulated Amazigo shells is given in Fig. 2(a), whereas the elements of the variance–covariance matrix are shown in Fig. 2(b). Since $i_{cl} = 6$, it is seen that on the diagonal at $i = j = i_{cl}$ the elements of the variance–covariance matrix reach a maximum. This maximum corresponds to the well-known peak in the spectral density (eqn 4) used by Amazigo in his analysis of the infinite shell.

It should be noticed that for sufficiently long shells the number of half-waves associated with the classical buckling mode $i_{cl} \gg 1$. Then ω_i tends to the continuous spatial frequency ω and in the expression for Ω_i (see eqn 41) the second and the third terms become vanishingly small in comparison with the leading term $\beta \bar{U}_i$. Thus as $L \to \infty$, σ_{ii} in eqn (40) reduces to the spectral density $\bar{S}_{w_0}(\omega)$ used by Amazigo for the infinite shell (see eqn 4). The extra factor of 4 is due to the fact that the half-wave cosine representation was employed for $\varphi_i(x)$ in deriving eqn (40) instead of the complex representation used by Amazigo. Further, as can be seen from Fig. 2(b), some off-diagonal terms $\sigma_{ij} (i \neq j)$ are different from zero. However, it can easily be shown using the expressions given in eqn (41) that as $L \to \infty$ the off-diagonal terms approach zero.

When comparing the results of the Monte Carlo Method for the mean buckling load with the prediction based on eqns (1) or (2), then according to the Kolmogorov–Smirnov test of goodness of fit [20] at a level of significance of 0.05 the critical value of the maximum absolute difference between the unknown theoretical and the obtained simulated distributions of the buckling loads is $1.36/\sqrt{100} = 0.136$. The variance of the simulated initial imperfections was

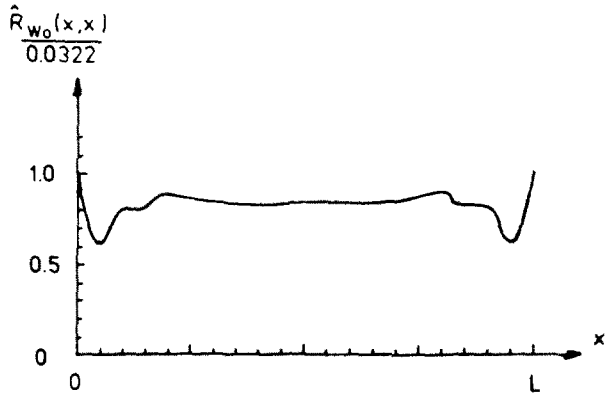

Fig. 1. Recalculated variance of "Amazigo's shell' (exponential–cosine autocorrelation function).

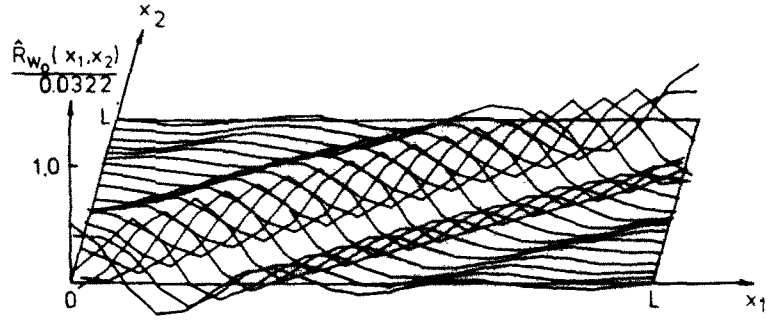

a. The back-calculated autocovariance function

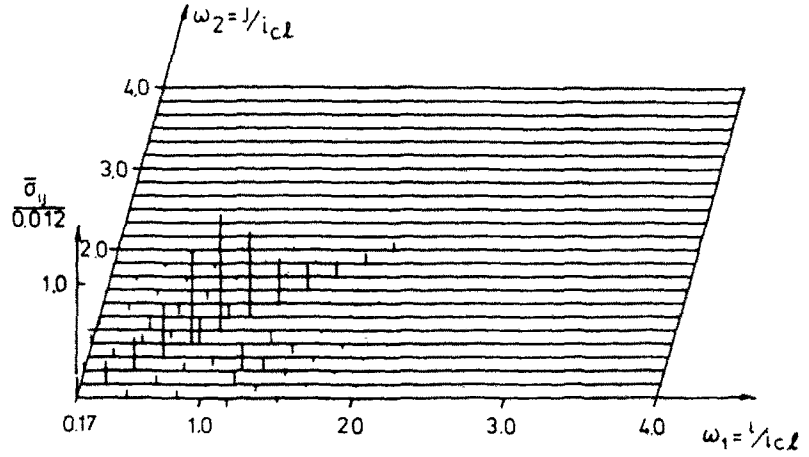

b. The elements of the variance-covariance matrix

Fig. 2. Statistical properties of the simulated 100 Amazigo shells.

fixed at $\delta^2 = 0.005$. The histogram of the buckling loads and the reliability function are shown in Figs. 3(a), (b), respectively. The nondimensional buckling loads λ were distributed between 0.376 and 0.886, so that the design buckling load at the required reliability, 0.98 say, equals 0.37. Obviously, the design buckling load associated with the high level of required reliability is a more powerful design criterion than the mean buckling load.

The mean buckling load possessed by the "created" shells is 0.608. Formula (1) by Amazigo[2] predicts 0.468 and formula (2) by Amazigo and Budiansky[3] yields 0.602. As is seen the mean buckling load given by eqn (2) is much more reliable than the one predicted by eqn (1) This is in agreement with the conjecture made in Ref. [3].

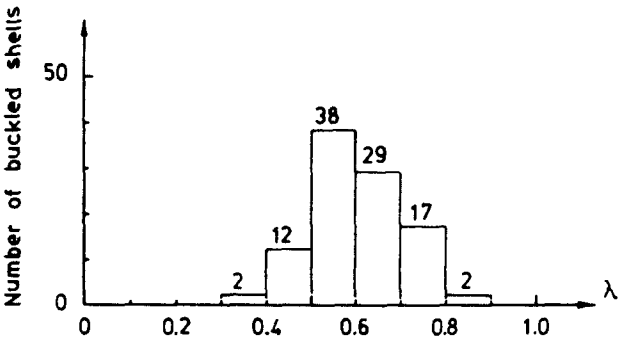

a. Histogram of the nondimensional buckling loads λ

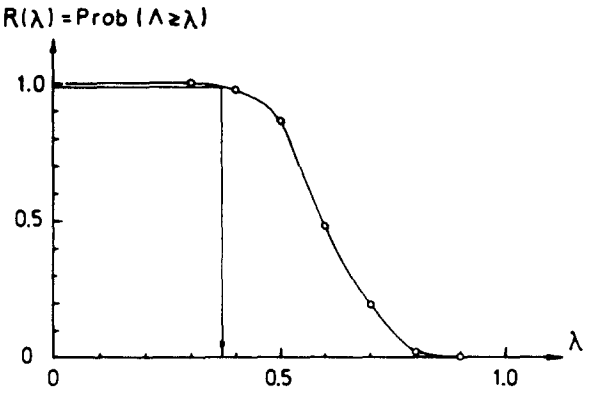

b. Calculated reliability function

Fig. 3. The reliability function associated with the simulated 100 Amazigo shells.

It should be remarked here that in the present work no use was made of the ergodicity assumption adopted in Refs. [2, 3], but ensemble averaging was employed to find the characteristics of the buckling load which turns out to be a random variable. Also, for the Monte Carlo simulation a shell of finite length was used and not an infinite one as in Refs. [2, 3].

4. SIMULATION OF RANDOM INITIAL IMPERFECTIONS FROM MEASURED DATA

The techniques for measuring the initial imperfections of shells are well established (see, e.g. Ref. [21]) and the results are collected in Refs. [22, 23]. The techniques employed measure the deviation of the shell outer surface relative to an imaginary cylindrical reference surface (the "perfect shell" associated with the imperfect shell under consideration). Consider, e.g. cylindrical shells of $L = 176.02$ mm, $R = 101.6$ mm, $t = 0.1160$ mm, manufactured by electroplating from pure copper, and tested in a controlled end-displacement type compression testing machine. We can visualize that a suitable stock of such shells, referred to as the A-shells[23], is available. Due to the very nature of the manufacturing process, each realization of the shell will have a different initial shape which cannot be predicted in advance. The imperfections represent deviations of the initial shape from the perfect circular cylinder amounting to a fraction of the wall thickness. They can be picked up and recorded by the special experimental set-up developed at Caltech[21]. The scanning device, moving in both the axial and the circumferential directions, yields a complete surface map of the shells. Any two shells produced by the same manufacturing process may have totally different imperfection profiles as can be seen from the three-dimensional plot of initial imperfections, shown in Fig. 4. Measured imperfection surfaces are represented by different Fourier series. The integrals involved in the determination of the Fourier coefficients are carried out numerically using the

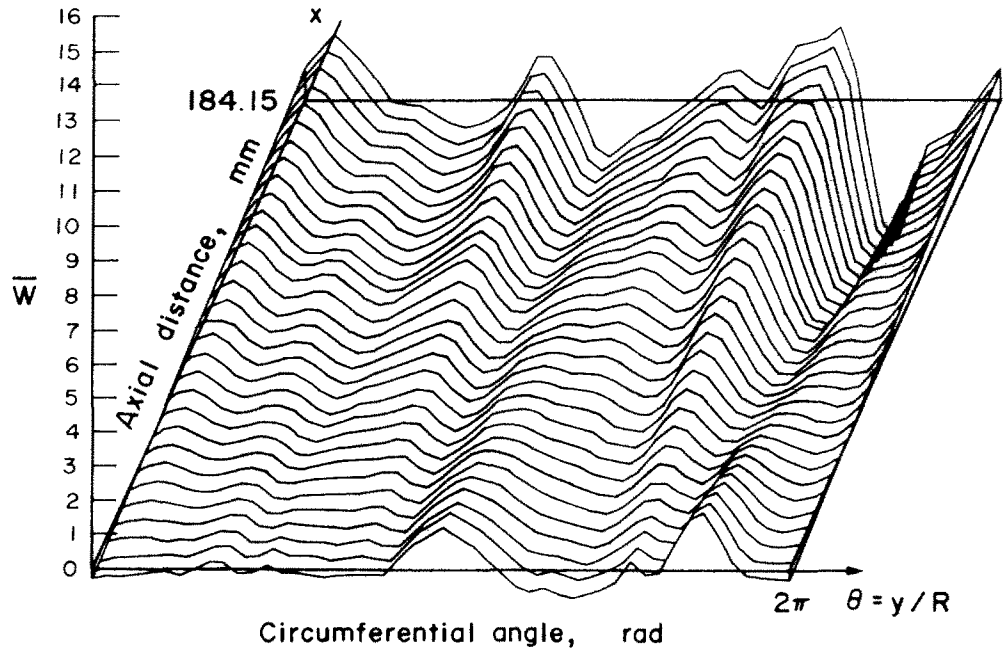

(a) Shell A–12[21]

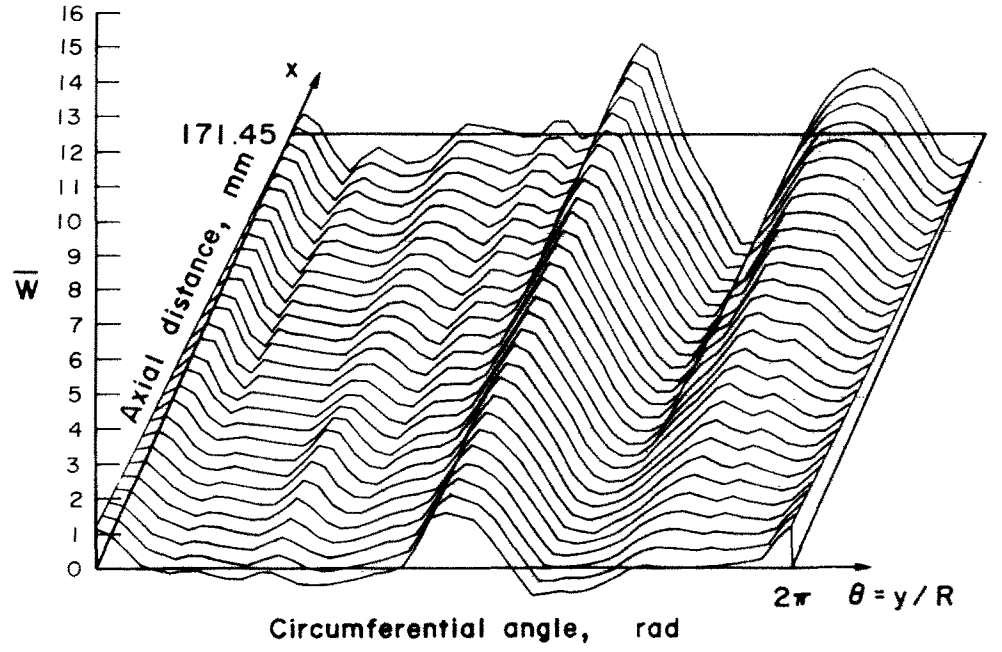

(b) Shell A–13[23]

Fig. 4. Three-dimensional plots of measured initial imperfections.

trapezoidal rule. The axisymmetric Fourier coefficients $a_i^{(m)}$ of the different A-shells are listed in Table 1. Now we are looking at the $a_i^{(m)}$'s as realizations of the random variable A_i in eqn (10). Then the sample mean is estimated as

$$\tilde{A}_i^{(e)} = \frac{1}{N} \sum_{m=1}^{N} a_i^{(m)} \tag{42}$$

where N is number of sample shells.

The elements σ_{ij} of the variance–covariance matrix are estimated as

$$\sigma_{ij}^{(e)} = \frac{1}{N-1} \sum_{m=1}^{N} [a_i^{(m)} - \tilde{A}_i^{(e)}][a_j^{(m)} - \tilde{A}_j^{(e)}] \tag{43}$$

which is an unbiased estimate.

The estimates of the mean initial imperfection function and of the autocovariance functions become, respectively (see eqns 11 and 13)

$$\tilde{W}_0^{(e)}(x) = \sum_i \tilde{A}_i^{(e)} \varphi_i(x)$$

$$R_{W_0}^{(e)}(x_1, x_2) = \sum_i \sum_j \sigma_{ij}^{(e)} \varphi_i(x_1) \varphi_j(x_2). \tag{44}$$

Since $[\Sigma] = [\sigma_{ij}^{(e)}]$ is a positive-semidefinite matrix, therefore according to Sylvester's theorem [24] all principal minor determinants associated with matrix $[\Sigma]$ are non-negative. The same property must be possessed by the estimate $[\Sigma^{(e)}]$. This property is used in order to "correct" initial values of $\sigma_{ij}^{(e)}$. If, for example, the r-th order principal minor determinant is non-negative

$$\begin{vmatrix} \sigma_{11}^{(e)} & \cdots & \sigma_{1r}^{(e)} \\ \vdots & & \\ \sigma_{r1}^{(e)} & \cdots & \sigma_{rr}^{(e)} \end{vmatrix} \geqq 0$$

but the $(r+1)$-th order principal minor determinant is negative

$$\begin{vmatrix} \sigma_{11}^{(e)} & \cdots & \sigma_{1r}^{(e)} & \sigma_{1,r+1}^{(e)} \\ \vdots & & & \\ \sigma_{r1}^{(e)} & \cdots & \sigma_{rr}^{(e)} & \sigma_{r,r+1}^{(e)} \\ \sigma_{r+1,1}^{(e)} & \cdots & \sigma_{r+1,r}^{(e)} & \sigma_{r+1,r+1}^{(e)} \end{vmatrix} < 0$$

then we perturb elements of the last column and row by some value x, so that the corrected $(r+1)$-th order principal minor determinant is positive

$$\begin{vmatrix} \sigma_{11}^{(e)} & \cdots & \sigma_{1r}^{(e)} & \sigma_{1,r+1}^{(e)} + x \\ \vdots & & & \\ \sigma_{r1}^{(e)} & \cdots & \sigma_{rr}^{(e)} & \sigma_{r,r+1}^{(e)} + x \\ \sigma_{r+1,1}^{(e)} + x & \cdots & \sigma_{r+1,r}^{(e)} + x & \sigma_{r+1,r+1}^{(e)} + x. \end{vmatrix} > 0$$

This "correction" can be used if $\max_j \sigma_{j,r+1}^{(e)} + x$ lies within the confidence interval for the element matrix $\sigma_{j,r+1}^{(e)}$, and, moreover, if $x \ll \max_j \sigma_{j,r+1}^{(e)}$.

Having the estimates of $\tilde{A}_i^{(e)}$ and $\sigma_{ij}^{(e)}$, we are proceeding to the simulation of the initial imperfections, as described in the previous section. Instead of $\{\tilde{A}\}$ and $[\Sigma]$ in eqns (34) and (35) we use $\{\tilde{A}^{(e)}\}$ and $[\Sigma^{(e)}]$, respectively. As a result we obtain the desired number $M > N$ initial imperfection profiles, which are statistically "equivalent" to the initial sample of N shells.

In order to check the simulation procedure, the autocovariance function of the simulated sample of shells, defined as

$$R_{W_0}^{(s)}(x_1, x_2) = \sum_m \sum_n \sigma_{ij}^{(s)} \varphi_i(x_1) \varphi_j(x_2) \tag{45}$$

with

$$\sigma_{ij}^{(s)} = \frac{1}{M-1} \sum_{m=1}^{M} [a_i^{(s)(m)} - \tilde{A}_i^{(s)}][a_j^{(s)(m)} - \tilde{A}_j^{(s)}] \tag{46}$$

must be compared with the autocovariance function of the initial sample $R_{W_0}^{(e)}$. The variance–covariance matrix for the group of A-shells is given in Appendix A and its elements are displayed in Fig. 5. The autocovariance function estimated from the measured data is displayed in Fig. 6. The autocovariance function of the simulated sample turns out to be indistinguishable from that of the measured initial sample. The estimated variance of the measured initial imperfection vs the axial coordinate is shown in Fig. 7.

A group of B-shells[23] was also considered. These shells were manufactured by putting pieces of thick-walled, seamless, brass tubes onto a mandrel and then machining them to the desired wall thicknesses. The average dimensions of this group of shells are $L = 134.37$ mm, $R = 101.6$ mm, $t = 0.2007$ mm and $\nu = 0.3$. The autocovariance function estimated from the measured data is displayed in Fig. 8. Also in this case the autocovariance function of the simulated sample showed excellent agreement with that of the measured initial sample. The elements of the variance–covariance matrix are given in Appendix B and are displayed in Fig. 9. The estimated variance of the measured initial data vs the axial coordinate is depicted in Fig. 10. As it is readily seen from Figs. 7 and 10, the variances associated with the A- and B-shells are non-uniform. This implies that their initial imperfections form nonhomogeneous random fields.

Note that $i_{cl} = 30$ for the group of A-shells and $i_{cl} = 17$ for the group of B-shells.

As can be seen from Figs. 5 and 9 (or from the numerical values in Appendices A and B) the Fourier coefficients of the axisymmetric part of the initial imperfections "peak" near $\omega = 0$ and become vanishingly small near $\omega = 1$. That means that the variance–covariance matrices of the shells investigated are dominated by the lower order modes and not by the classical axisymmetric buckling mode.

Next we are proceeding to the second step of the Monte Carlo Method: evaluation of the buckling load for each "created" shell.

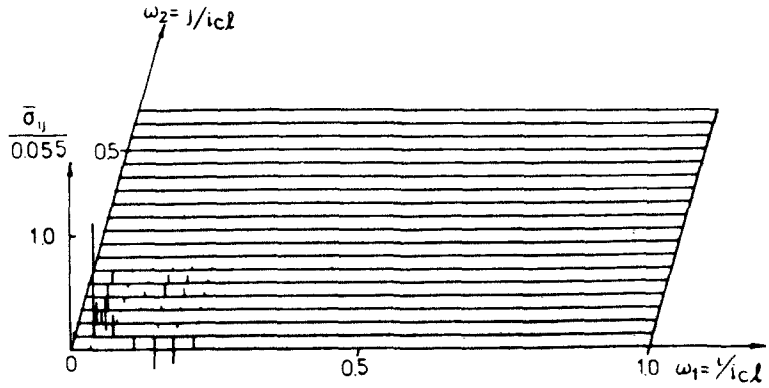

Fig. 5. Elements of the variance–covariance matrix $[\Sigma^e]$ of the group of A-shells.

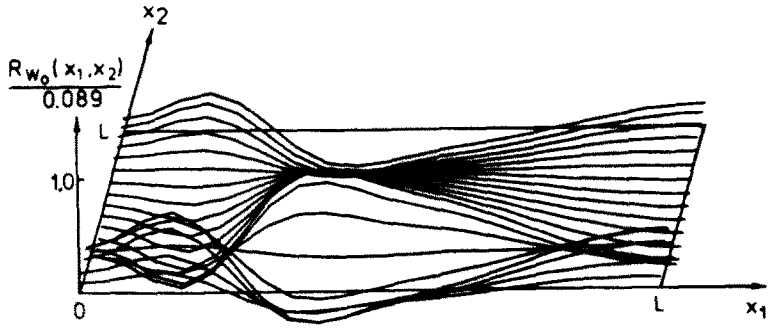

Fig. 6. The estimated autocovariance function of the axisymmetric part of the measured initial imperfections for the group of *A*-shells.

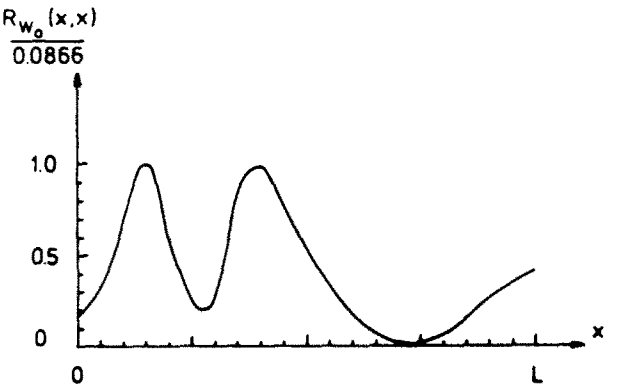

Fig. 7. Estimated variance of the measured initial imperfections as a function of the axial coordinate for the group of *A*-shells.

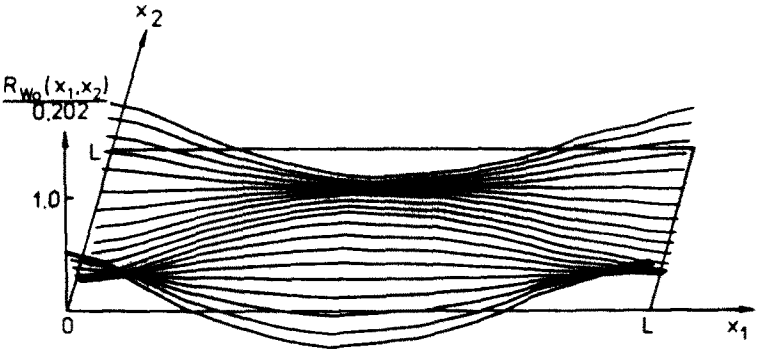

Fig. 8. The estimated autocovariance function of the axisymmetric part of the measured initial imperfections for the group of *B*-shells.

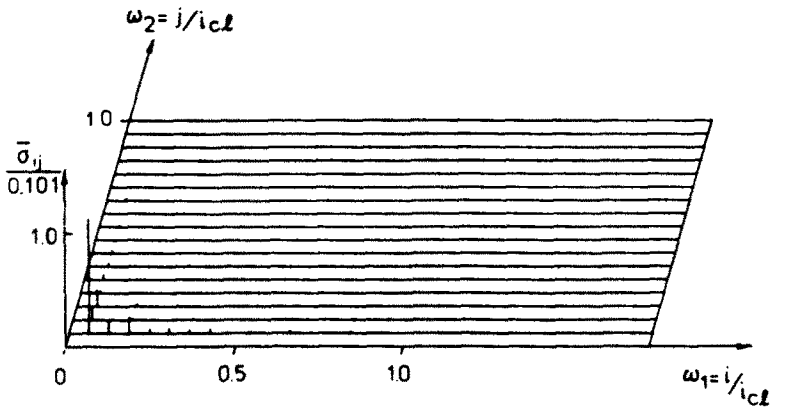

Fig. 9. Elements of the variance–covariance matrix $[\Sigma^e]$ of the group of *B*-shells.

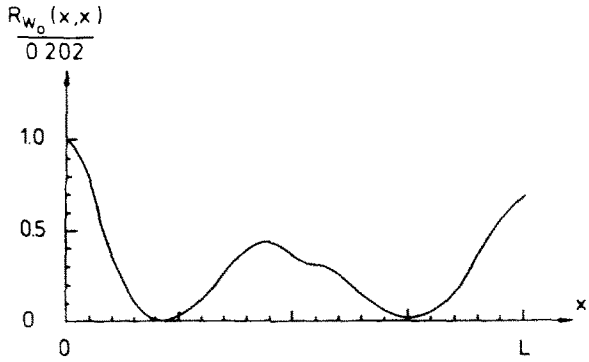

Fig. 10. Estimated variance of the measured initial imperfections as a function of the axial coordinate for the group of B-shells.

5. COMPUTATION OF THE BUCKLING LOADS

The buckling loads are calculated by making use of Koiter's special theory[25]. We are considering a cylindrical shell with an axisymmetric initial imperfection of the form

$$w_0(x) = t\bar{\xi}_i \cos\frac{i\pi x}{L} \tag{47}$$

where $\bar{\xi}_i$ denotes the magnitude of the imperfection as a fractional value of the shell thickness t and i is an integer denoting the number of half waves in the axial direction. Using Koiter's special non-linear theory one can derive a relationship between the nondimensional axial load level λ (at which the resulting fundamental equilibrium state bifurcates into an asymmetric deformation pattern) and the imperfection amplitude $\bar{\xi}_i$. It one assumes the following buckling mode

$$w(x, y) = tC_{kl} \sin\frac{k\pi x}{L} \cos\frac{ly}{R} \tag{48}$$

where k and l are integers denoting the number of half waves and the number of full waves in the axial and in the circumferential directions, respectively, then the following non-linear transfer function between λ and $\bar{\xi}_i$ is obtained.

$$(\lambda_{c_i} - \lambda)^2(\lambda_{c_{kl}} - \lambda) + (\lambda_{ci} + \lambda)\frac{c}{2}\frac{\beta_l^2}{\alpha_k^2}\left[\lambda + \lambda_{c_i}\frac{8\alpha_k^4}{(\alpha_k^2 + \beta_l^2)^2}\right]\bar{\xi}_i\delta_{ij} + 8c^2\alpha_k^2\beta_l^4$$
$$\times\left[\frac{1}{(9\alpha_k^2 + \beta_l^2)^2} + \frac{1}{(\alpha_k^2 + \beta_l^2)^2}\right]\lambda_{ci}^2\bar{\xi}_i^2 = 0 \tag{49}$$

where

$$\lambda_{c_i} = \frac{1}{2}\left(\alpha_i^2 + \frac{1}{\alpha_i^2}\right), \quad \lambda_{c_{kl}} = \frac{1}{2}\left[\frac{(\alpha_k^2 + \beta_k^2)^2}{\alpha_k^2} + \frac{\alpha_k^2}{(\alpha_k^2 + \beta_l^2)^2}\right]$$
$$\alpha_i^2 = i^2\frac{Rt}{2c}\left(\frac{\pi}{L}\right)^2, \quad \alpha_k^2 = k^2\frac{Rt}{2c}\left(\frac{\pi}{L}\right)^2, \quad \beta_l^2 = l^2\frac{Rt}{2c}\left(\frac{1}{R}\right)^2 \tag{50}$$

and δ_{ij} is the Kronecker delta with $j = 2k$.

It is shown in Appendix E that eqn (49) can be reduced to eqn (5.2) of Ref. [25]. From eqn (49) for an imperfection sensitive structure $\bar{\xi}_i$ must be negative and i must be an even integer. The use of eqn (49) to calculate the critical buckling load for a given shell then proceeds as follows. Initially with $i = 2$, $k = 1$ (since $i = 2k$) and for different values of l eqn (49) is solved repeatedly and the lowest bifurcation buckling load λ is determined. Next the process is repeated with $i = 4, 6, \cdots$ until all the available imperfection harmonics have been tested.

The absolute minimum bifurcation buckling load is then identified as the critical buckling load for the shell under consideration.

Once the critical buckling loads for the large number of simulated shells ($M = 100$) are available, one can then proceed to calculate the histogram of the buckling loads and to determine the corresponding reliability function. Figures 11–14 display the histograms of the buckling loads and the calculated reliability functions for the group of A- and B-shells respectively. A comparison of Figs. 12 and 14 shows that the reliability of the B-shells is less than that of the A-shells, meaning that machining thin-walled shells out of thick-walled, seamless, brass tubes is a "rougher" procedure than electroplating.

Note that the mean buckling load for the simulated sample of A-shells is 0.946, whereas for the B-shells is 0.724. These loads are considerably higher than the experimentally observed mean buckling loads for the corresponding initial samples (0.643 for the A-shells, 0.592 for the B-shells). The reason is, that as has been pointed out in Ref. [26] for accurate buckling load predictions also the asymmetric imperfections must be taken into account. The study of the effect of general, non-axisymmetric imperfections is under way and will be published elsewhere. Thus this work can be viewed as the first step towards such a general analysis.

6. CHECK OF THE MONTE CARLO METHOD IN A CASE CAPABLE OF EXACT SOLUTION

The question arises: "What is the accuracy of the Monte Carlo Method?" In order to provide a check of this method when applied to shell structures let us consider a case capable of an exact solution. If one assumes that the initial imperfections are of the form

$$w_0(x) = t\bar{\xi}\cos i_{cl}\frac{\pi x}{L} \tag{51}$$

where $\bar{\xi}$ is a random variable $\bar{X}$ with given probability distribution density $f_{\bar{X}}(\bar{\xi})$, then the shape

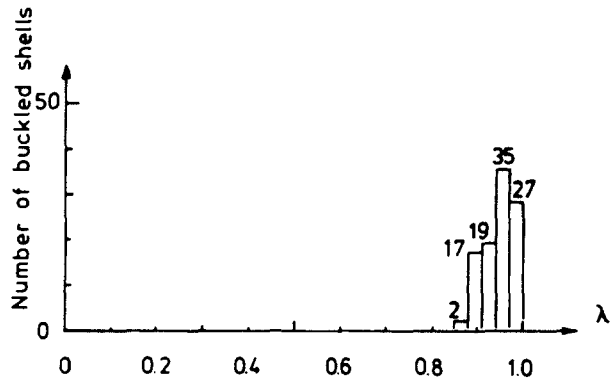

Fig. 11. Histogram of the nondimensional buckling loads λ (Group of A-shells[23]).

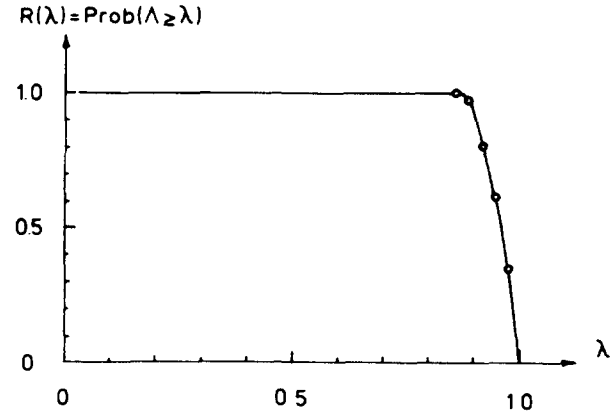

Fig. 12. Calculated reliability function vs the nondimensional buckling load λ (Group of A-shells[23]).

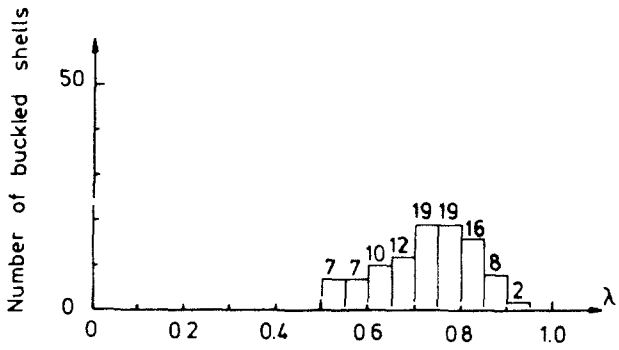

Fig. 13. Histogram of the nondimensional buckling loads λ (Group of B-shells[23]).

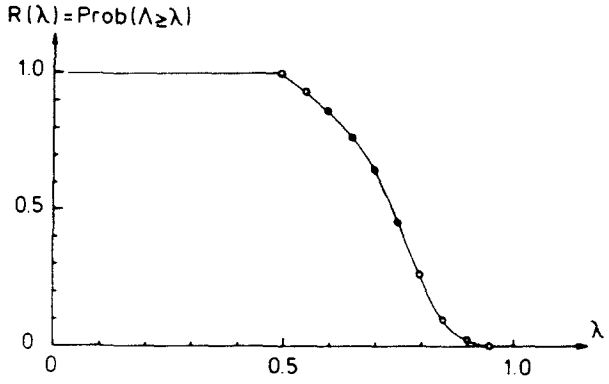

Fig. 14. Calculated reliability function vs the nondimensional buckling load λ (Group of B-shells[23]).

of the axisymmetric imperfection coincides with the axisymmetric buckling mode of the perfect shell. Hence $\lambda_{c_i} = 1$, $\alpha_i^2 = 1$, $\alpha_k^2 = 1/4$ (since $i = 2k$) and eqn (49) reduces to

$$(1-\lambda)^2(\lambda_{c_{kl}} - \lambda) + (1-\lambda)2c\beta_l^2\left[\lambda + \frac{8}{(1+4\beta_l^2)^2}\right]\bar{\xi} + 32c^2\beta_l^4\left[\frac{1}{(9+4\beta_l^2)^2} + \frac{1}{(1+4\beta_l^2)}\right]\bar{\xi}^2 = 0. \tag{52}$$

It is shown in Appendix E that eqn (52) is equivalent to eqn (5.4) of Ref. [25]. Equation (52) then represents the non-linear transfer function between λ and $\bar{\xi}$. If the amplitude of the imperfection $\bar{\xi}$ is a random variable $\bar{X}$ then also the buckling load λ will be a random variable Λ. Thus eqn (52) becomes

$$(1-\Lambda)^2(\lambda_{c_{kl}} - \Lambda) - (1-\Lambda)2c\beta_l^2\left[\Lambda + \frac{8}{(1+4\beta_l^2)^2}\right]|\bar{X}| + 32c^2\beta_l^4\left[\frac{1}{(9+4\beta_l^2)^2} + \frac{1}{(1+4\beta_l^2)}\right]\bar{X}^2 = 0 \tag{53}$$

The minus sign has been introduced (as discussed earlier) in order to obtain an imperfection sensitive structure. The reliability is then defined as the probability that the buckling load Λ will be greater or equal to some specified value α. As it follows from eqn (53) this is equivalent to the probability that the absolute value of the imperfection $\bar{X}$ be less than or equal to some value $\bar{\xi}^*$, where $\bar{\xi}^*$ is the smallest root of the transfer function (53) for the specified value of $\Lambda = \alpha$.

It should be noted here that eqn (53) contains as a free parameter l, the number of full waves in the circumferential direction. Thus finding the smallest root $\bar{\xi}^*$ for a given value of $\Lambda = \alpha$ involves repeated solution of eqn (53) for different values of l.

If we now introduce the distribution function $F_{\bar{X}}(\bar{\xi})$ then by definition

$$\Pr\{\bar{X} \leqq \bar{\xi}^*\} = F_{\bar{X}}(\bar{\xi}^*) = \int_{-\infty}^{\bar{\xi}^*} f_{\bar{X}}(\bar{\xi})\,\mathrm{d}\bar{\xi} \tag{54}$$

and the reliability can be written as

$$R(\alpha) = \text{Prob}\{\Lambda \geqq \alpha\}$$

$$= \text{Prob}\{|\bar{X}| \leqq \bar{\xi}^*\} = \int_{-\bar{\xi}^*}^{\bar{\xi}^*} f_{\bar{X}}(\bar{\xi})\,\mathrm{d}\bar{\xi} = F_{\bar{X}}(\bar{\xi}^*) - F_{\bar{X}}(-\bar{\xi}^*) \tag{55}$$

Thus the reliability equals the integral of the initial imperfection amplitude probability density $f_{\bar{X}}(\bar{\xi})$ over the interval $(-\bar{\xi}^*, \bar{\xi}^*)$.

If one now further assumes that the random variable $\bar{X}$ is normally distributed with mean $m_{\bar{X}}$ and variance $\sigma_{\bar{X}}^2$, then its probability density is given by

$$f_{\bar{X}}(\bar{\xi}) = \frac{1}{\sigma_{\bar{X}}\sqrt{(2\pi)}}\,\mathrm{e}^{-1/2((\bar{\xi}-m_{\bar{X}})/\sigma_{\bar{X}})^2} \tag{56}$$

and we get from eqn (55) the following closed form solution for the reliability:

$$R(\alpha) = \frac{1}{2}\left\{\text{erf}\left(\frac{\bar{\xi}^* - m_{\bar{X}}}{\sigma_{\bar{X}}\sqrt{2}}\right) - \text{erf}\left[\frac{-(\bar{\xi}^* - m_{\bar{X}})}{\sigma_{\bar{X}}\sqrt{2}}\right]\right\} = \text{erf}\left(\frac{\bar{\xi}^* - m_{\bar{X}}}{\sigma_{\bar{X}}\sqrt{2}}\right) \tag{57}$$

where erf (x) is an error function defined as

$$\text{erf}\,(x) = \frac{2}{\sqrt{\pi}}\int_0^x \mathrm{e}^{-t^2}\,\mathrm{d}t. \tag{58}$$

The reliability calculation is illustrated in Fig. 15 where the shaded area equals the reliability of the shell at the nondimensional load level α.

For the sake of comparison 1089 imperfect shells were "created". Their dimensions were $L = 141.0$ mm, $R = 101.6$ mm, $t = 0.2634$ mm and $\nu = 0.3$ so that $i_{cl} = 16.0$. The shape of the imperfections coincided with the classical axisymmetric buckling mode and their amplitudes were normally distributed random variables with a mean of $m_{\bar{X}} = 0.1$ and a standard deviation of $\sigma_{\bar{X}} = 0.05$. The histogram of the buckling loads is shown in Fig. 16. The buckling loads were computed following the procedure outlined in the preceding section with eqn (52) in place of eqn (49). The reliability functions are shown in Fig. 17. The solid line indicates the analytical solution from eqn (57). The results of the Monte Carlo Method are shown by circles. The agreement between the simulated and the analytical results is excellent.

7. CONCLUSIONS

It has been demonstrated that the Monte Carlo Method can be used successfully for the investigation of the stochastic imperfection sensitivity of axially compressed cylindrical shells with axisymmetric initial imperfections. The authors believe that the reliability function—the final product of such an analysis—represents a more powerful design criterion than the ones based on deterministic or mean buckling load formulas.

Computation of the variance–covariance matrices of the Fourier coefficients as ensemble averages of the experimentally determined values have shown that the measured initial imperfections of finite shells are nonhomogeneous. Thus the ergodicity assumption used by many investigations is not applicable.

As has been seen the results of the existing initial imperfection data banks can be incorporated directly into the Monte Carlo Method. Thus the results presented in this paper further reinforce the need for compiling extensive experimental information on imperfections classified according to the manufacturing processes.

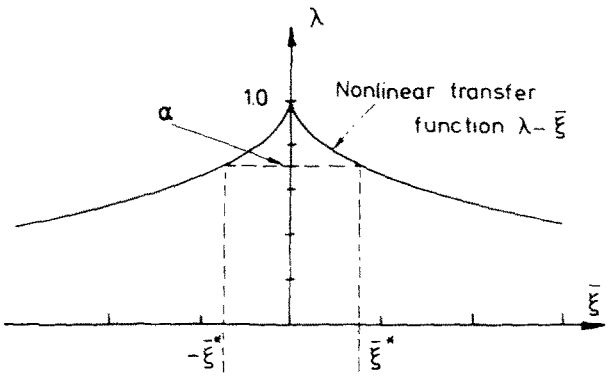

a. Critical buckling load λ vs imperfection amplitude $\bar{\xi}$

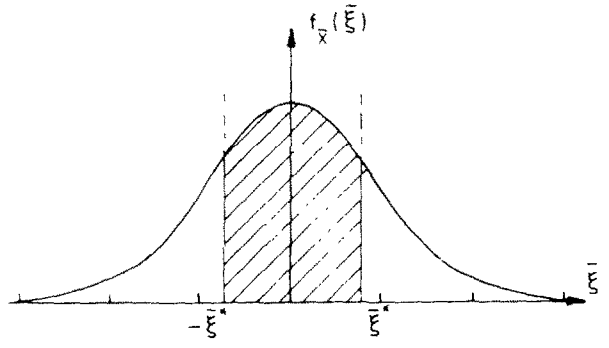

b. Probability density of the initial imperfection amplitude

Fig. 15. Illustration of the reliability calculation.

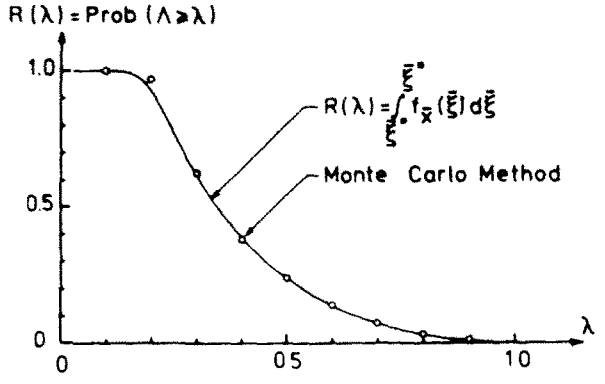

Fig. 16. Histogram of the nondimensional buckling loads λ.

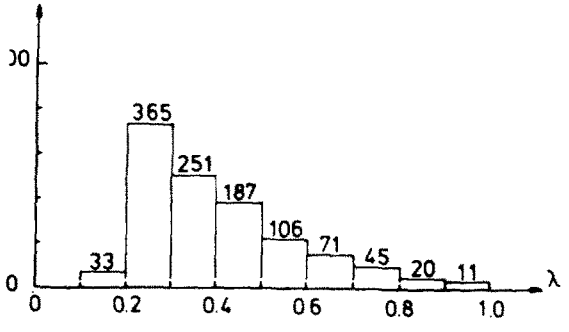

Fig. 17. Comparison of analytical reliability function with results of the Monte Carlo Method.

By the technique developed in Refs. [1, 17–19] and in this paper (once it has been extended to include general nonsymmetric imperfections), one can then calculate via the Monte Carlo Method the reliability functions associated with the different manufacturing processes. Thus finally, by this approach, the imperfections sensitivity concept can be introduced into the design procedure.

Acknowledgements—Part of this work has been performed at the Department of Aeronautical Engineering, Israel Institute of Technology, Haifa. It has been completed during the first author's sabbatical stay at the Department of Aerospace Engineering, Delft University of Technology. This aid and the warm and kind hospitality are gratefully acknowledged.

The authors also wish to express their appreciation to Miss Henny Schreuders for the skilful typing of the manuscript and to Mr. John Heijdra and to Mr. Kess Venselaar for the excellent drawings.

REFERENCES

1. I. Elishakoff, Buckling of a stochastically imperfect finite column on a nonlinear elastic foundation—a reliability study, *ASME J. Appl. Mech.* **46**, 411–416 (1979).
2. J. C. Amazigo, Buckling under axial compression of long cylindrical shells with random axisymmetric imperfections. *Quart. Appl. Mathematics* **26**, 537–566 (1969).
3. J. C. Amazigo and B. Budiansky, Asymptotic formulas for the buckling stresses of axially compressed cylinders with localized or random axisymmetric imperfections. *ASME J. Appl. Mech.* **39**, 179–184 (1972).
4. R. C. Tennyson, D. B. Muggeridge and R. D. Caswell, Buckling of circular cylindrical shells having axisymmetric imperfection distributions. *AIAA J.* **9**, 924–930 (1971).
5. J. Arbocz, The effect of initial imperfections in shell stability, *Thin Shell Structures: Theory, Experiment and Design* (Edited by Y. C. Fung and E. E. Sechler), pp. 205–245. Prentice-Hall, Englewood Cliffs, New Jersey (1974).
6. J. Roorda and J. S. Hansen, Random buckling behaviour in axially loaded cylindrical shells with axisymmetric imperfections. *J. Spacecraft* **9**, 88–91 (1972).
7. W. T. Koiter, On the stability of elastic equilibrium (in Dutch) Ph.D.-Thesis, Delft University, H. J. Paris, Amsterdam, English Translations, (a) NASA TTF-10, 833, 1967, (b) AFFDL-TR-70-20, 1970.
8. J. Roorda, Buckling of shells: an old idea with a new twist, *ASCE J. Engng Mech. Div.* **98**(EM3), 531–538 (1972).
9. L. J. Hart-Smith, Buckling of thin cylindrical shells under axial compression, *Int. J. Solids Structures*, **12**, 299–313 (1970).
10. V. I. Weingarten, E. J. Morgan and P. Seide, Elastic stability of thin-walled cylindrical and conical shells under axial compression, *AIAA J.* **3**, 500–505 (1965).
11. B. P. Makaroff, Statistical analysis of nonideal cylindrical shells, *Izvestija Akademii Nauk SSR, Mekhanika Tverdogo Tela* **5**(1), 97–104 (1970). In Russian.
12. B. P. Makaroff, Statistical analysis of stability of imperfect cylindrical shells. *7th All-Union Conf. on the Theory of Plate and Shells, Dnepropetrovsk, Proceedings*, 387–391 (1969). In Russian.
13. R. Fersht, Buckling of cylindrical shells with random imperfections. *Thin Shell Structures: Theory, Experiment and Design* (Edited by Y. C. Fung and E. E. Sechler), pp. 325–341. Prentice-Hall, Englewood Cliffs, New Jersey (1974).
14. J. Hansen, General random imperfections in the buckling of axially loaded cylindrical shells. *AIAA J.* **15**, 1250–1256 (1977).
15. J. Hansen, Influence of general imperfections in axially loaded cylindrical shells. *Int. J. Solids Structures* **11**, 1223–1233 (1975).
16. J. Arbocz and J. G. Williams, Imperfection surveys on a 10 ft diameter shell structure. *AIAA J.* **15**, 949–956 (1977).
17. I. Elishakoff, Simulation of space-random fields for solution of stochastic boundary-value problems. *J. Acoustical Society of America* **65**, 399–403 (1979).
18. I. Elishakoff, Impact buckling of thin bar via Monte Carlo method. *ASME J. Appl. Mech.* **45**, 586–590 (1978).
19. I. Elishakoff, Hoff's problem in a probabilistic setting. *ASME J. Appl. Mech.* **47**, 1–6 (1980).
20. F. J. Massey, Jr., The Kolmogorov–Smirnov test for goodness of fit. *J. Amer. Statist. Assoc.* **46**, 68–78 (1951).
21. J. Arbocz and C. D. Babcock, Jr., Experimental investigation of the effect of general imperfections on the buckling of cyclindrical shells. NASA CR-1163 (1968).
22. J. Singer, H. Abramovich and R. Yaffe, Initial imperfection measurements of integrally stringer-stiffened cylindrical shells. TAE Rep. 330, Department of Aeronautical Engineering, Technion, Israel Institute of Technology, Haifa, Israel, Dec. 1978.
23. J. Arbocz and H. Abramovich, The initial imperfection data bank at the Delft University of technology–Part I. Rep. LR-290, Department of Aerospace Engineering, Dec. 1979.
24. N. G. Chetaev, *The Stability of Motion*, Section 20. Pergamon Press, New York (1961).
25. W. T. Koiter, The effect of axisymmetric imperfections on the buckling of cylindrical shells under axial compression. Koninklijke Nederlandse Akademie van Wetenschappen (*Proc. Royal Netherlands Academy of Sciences*), Amsterdam, Series 13, Vol. 66, No. 5, pp. 265–279 (1963).
26. J. Arbocz and C. D. Babcock, Jr., Prediction of buckling loads based on experimentally measured initial imperfections. *Proc. IUTAM Symp. Buckling of Structures, Cambridge*, U.S.A., 1974 (Edited by B. Budiansky), Springer Verlag, Berlin (1976).
27. I. Elishakoff and J. Arbocz, Reliability of axially compressed cylindrical shells with random axisymmetric imperfections, Report LR-306, Department of Aerospace Engineering, Delft University of Technology, The Netherlands (Sept. 1980).

APPENDIX 1

Statistical properties of the group of A-*shells*

Table 1. First nine Fourier coefficients $a_i^{(m)}$ of the initial imperfections expanded as

$$w_0^{(m)}(x) = tW_0^{(m)}(x) = t\sum_{i=0}^{8} a_i^{(m)} \cos\frac{i\pi x}{L}$$

i \ shell	A-7	A-8	A-9	A-10	A-12	A-13	A-14
0	0.0176	0.0343	0.0226	0.0108	0.0023	0.0018	0.0029
1	0.0669	0.6534	0.0832	-0.0231	0.0158	0.0242	0.0662
2	-0.0164	0.1033	-0.0437	-0.0265	-0.0164	0.0095	0.0041
3	-0.0176	-0.0696	-0.0079	0.0054	0.0174	0.0006	0.0237
4	-0.0403	-0.1997	-0.0519	-0.0232	0.0092	0.0048	0.0013
5	-0.0031	-0.1637	0.0015	-0.0055	-0.0194	-0.0021	-0.0438
6	-0.0313	-0.0787	-0.0347	-0.0187	0.0062	-0.0047	-0.0349
7	-0.0050	-0.0092	-0.0080	-0.0106	0.0115	0.0060	0.0042
8	-0.0326	-0.0821	-0.0370	-0.0158	-0.0116	0.0038	-0.0041

for the group of A-shells ($R = 101.6$ mm, $t = 0.1160$ mm, $L = 176.02$ mm, $E = 1.0441 \times 10^5$ N/mm^2, $\nu = 0.3$, $i_{cl} = 30$).
Note: Here $w_0^{(m)}(x)$ is positive outward:

Table 2. Elements of the variance–covariance matrix $[\Sigma^{(e)}]$ for the group of A-shells

$[\Sigma^{(e)}] =$

i \ J	0	1	2	3	4	5	6	7
0	0.015	0.230	0.030	-0.035	-0.083	-0.046	-0.029	-0.008
1	0.230	5.530	1.031	-0.658	-1.644	-1.338	-0.556	-0.079
2	0.030	1.031	0.232	-0.113	-0.277	-0.270	-0.092	-0.005
3	-0.035	-0.658	-0.113	0.096	0.217	0.140	0.069	0.016
4	-0.083	-1.644	-0.277	0.217	0.533	0.375	0.180	0.039
5	-0.046	-1.338	-0.270	0.140	0.375	0.353	0.130	0.013
6	-0.029	-0.556	-0.092	0.069	0.180	0.130	0.074	0.016
7	-0.008	-0.079	-0.005	0.016	0.039	0.013	0.016	0.007

$\times 10^{-2}$

APPENDIX 2

Statistical properties of the group of B-*Shells*

Table B1: First fifteen Fourier coefficients $a_i^{(m)}$ of the initial imperfections expanded as

$$w_0^{(m)}(x) = tW_0^{(m)}(x) = t\sum_{i=0}^{14} a_i^{(m)} \cos\frac{i\pi x}{L}$$

i \ shell	B-1	B-2	B-3	B-4
0	0.0010	0.0028	0.0111	0.0080
1	-0.0333	-0.1889	-0.6231	0.1096
2	-0.0108	-0.0272	-0.0899	-0.0176
3	-0.0190	-0.0276	-0.0803	0.0407
4	0.0226	-0.0078	-0.0255	-0.0092
5	-0.0025	-0.0097	-0.0230	0.0132
6	0.0018	-0.0049	-0.0223	-0.0059
7	-0.0062	-0.0080	-0.0189	0.0120
8	0.0076	-0.0074	0.0052	-0.0125
9	-0.0050	0.0023	0.0053	0.0254
10	-0.0013	-0.0041	-0.0133	-0.0265
11	0.0015	-0.0007	-0.0033	0.0200
12	-0.0062	-0.0009	-0.0085	-0.0176
13	0.0084	-0.0031	0.0092	0.0103
14	0.0020	-0.0027	-0.0136	-0.0114

for the group of B-shells ($R = 101.6$ mm, $t = 0.2007$ mm, $L = 134.30$ mm, $E = 1.065 \times 10^5$ N/mm^2, $\nu = 0.3$, $i_{cl} = 17$). Note: Here $w_0^{(m)}(x)$ is positive outward:

Table B2. Elements of the variance–covariance matrix $[\Sigma^{(e)}]$ for the group of B-shells

$$[\Sigma^{(e)}] = \begin{array}{c|c} i \backslash j & \begin{matrix} 0 & 1 & 2 & 3 & 4 & 5 & 6 & 7 & 8 & 9 & 10 \end{matrix} \\ \hline \begin{matrix} 0 \\ 1 \\ 2 \\ 3 \\ 4 \\ 5 \\ 6 \\ 7 \\ 8 \\ 9 \\ 10 \end{matrix} & \begin{bmatrix} 0.002 & -0.079 & -0.013 & -0.006 & -0.008 & -0.002 & -0.004 & -0.001 & -0.0005 & 0.003 & -0.004 \\ -0.079 & 10.059 & 1.095 & 1.489 & 0.398 & 0.454 & 0.279 & 0.364 & -0.160 & 0.145 & -0.070 \\ -0.013 & 1.095 & 0.132 & 0.145 & 0.057 & 0.044 & 0.036 & 0.033 & -0.013 & 0.003 & 0.005 \\ -0.006 & 1.489 & 0.145 & 0.247 & 0.035 & 0.074 & 0.033 & 0.063 & -0.034 & 0.041 & -0.028 \\ -0.008 & 0.398 & 0.057 & 0.035 & 0.040 & 0.012 & 0.018 & 0.006 & 0.006 & -0.012 & 0.012 \\ -0.002 & 0.454 & 0.044 & 0.074 & 0.012 & 0.023 & 0.010 & 0.019 & -0.009 & 0.012 & -0.008 \\ -0.004 & 0.279 & 0.036 & 0.033 & 0.018 & 0.010 & 0.010 & 0.007 & -0.002 & -0.002 & 0.004 \\ -0.001 & 0.364 & 0.033 & 0.063 & 0.006 & 0.019 & 0.007 & 0.016 & -0.009 & 0.012 & -0.009 \\ -0.0005 & -0.160 & -0.013 & -0.034 & 0.006 & -0.009 & -0.002 & -0.009 & 0.009 & -0.010 & 0.007 \\ 0.003 & 0.145 & 0.003 & 0.041 & -0.012 & 0.012 & -0.002 & 0.012 & -0.010 & 0.017 & -0.014 \\ -0.004 & -0.070 & 0.005 & -0.028 & 0.012 & -0.008 & 0.004 & -0.009 & 0.007 & -0.014 & 0.013 \end{bmatrix} \end{array} \times 10^{-2}$$